Multi-Metal Adsorption of Lead (II), Cadmium (II), and Manganese (II) Ions from Simulated Solution onto HDTMA-Br Modified Dijah-Monkin Bentonite Clay

Umar Omeiza Aroke [1], Olukayode Gideon Oloyede [1], Saidat Olanipekun Giwa [1]

[1] *Abubakar Tafawa Balewa University*
Tafawa Balewa Way, P. M. B. 0248, Bauchi, 740272, Nigeria

DOI: 10.22178/pos.105-33

LCC Subject Category: QD1-999

Received 21.05.2024
Accepted 25.06.2024
Published online 30.06.2024

Corresponding Author:
Olukayode Gideon Oloyede
oloyede.gideon@gmail.com

Abstract. In this study, Dijah-Monkin bentonite clay was modified with a cationic surfactant hexadecyltrimethylammonium bromide (HDTMA-Br) at the level of twice the cation exchange capacity (CEC) and applied in adsorption to obtain the optimal conditions for the removal of lead (II), cadmium (II) and manganese (II) from a solution. The Box-Behnken design matrix comprised particle size of clay, initial metal ion concentration, and contact time as the independent variables, with the heavy metals' adsorption capacities and percentage removals as the responses. The experimental results fit linear models for the adsorption capacity and quadratic models for the percentage removal. Also, only the particle size and initial concentration significantly affected the responses. However, the effect of contact time was significant for cadmium removal, suggesting that the adsorption of cadmium ion on the adsorbent increases with increased contact time; this is due to high cadmium cation hydration energy of -1807 kJ/mol^{-1} compared to lead and manganese with -1481 kJmol^{-1}, -1760 kJmol^{-1} respectively. Furthermore, the model equations for the responses were developed, and the optimum adsorption condition for the multi-metal adsorption that maximised the adsorption capacity and the percentage removal was obtained to be 150 µm particle size, 50 mg/l initial concentration over 171 minutes.

Keywords: Adsorption; Analysis of Variance; Response Surface Methodology; Box-Behnken, Dijah-Monkin Bentonite Clay; Hexadecyltrimethylammonium bromide; Multi-metal; Zing-North East Nigeria.

INTRODUCTION

A healthy and rising human population necessitates the availability of drinking water. However, the widespread use of chemicals and increased industrialisation steadily increase the burden of toxins in drinking water [1]. Heavy metals are among the most common pollutants found in wastewater, and even at low concentrations, they can be hazardous to humans and animals [2]. Managing pollution caused by heavy metals has recently become a significant issue, particularly in developing countries.

Heavy metals are toxic or poisonous metals and metalloid elements with a relatively high density of 3.5 to 7 g/cm^3. Many such metals are present extensively in the earth's crust and are non-biodegradable [3]. Air, food and water are absorbed into the human body [2]. Heavy metals are among the most prevalent pollutants identified in wastewater.

However, given the challenge of preventing the drainage of these pollutants into water supplies, implementing effective purification technologies is a relatively efficient way to maintain safer/cleaner bodies of water. Multiple treatment methods have been studied for water purification, such as using clay/modified clay, biological or inert content (bio-sorbent) for sorption, flocculation-coagulation by various chemical agents, etc. [4]. Adsorption is preferred among many techniques because it is cost-effective, highly accurate, energy-efficient, versatile, and can quickly recycle spent adsorbent [5]. Heavy metals differ

widely in their chemical properties and are used extensively in electronics, machines and the artefacts of everyday life, as well as in high-tech applications. As a result, they can enter into the aquatic and food chains of humans and animals from various anthropogenic sources and the natural geochemical weathering of soil and rocks [2]. Heavy metals in wastewater include lead, cadmium, arsenic, mercury, zinc, chromium, nickel, copper, vanadium, platinum, silver, gold, selenium and uranium [6]. Nearly all of these metals have no known biological function in living organisms. At the same time, some, like copper, zinc, and nickel, are considered essential below 0.005 mg/l but are toxic when increased beyond the permissible unit [7].

Cadmium is one of the most toxic elements in the food chain and is the cause of kidney disorders and bone disease. Thus, cadmium is not essential for biological systems. It is used to manufacture nickel-cadmium batteries, plastics and pigments. Phosphate fertilisers and waste dumping are both routes for cadmium transference into the environment. Concern regarding the role and toxicity of cadmium in the environment is increasing because it can be highly toxic to humans and animals. Smoking cigarettes is one of the sources of cadmium poisoning in humans [2]. The permissible limit for cadmium in drinking water is 0.003 mg/l [8].

Lead is another toxic heavy metal widely used in industrial applications such as batteries, printing, pigments, fuels, photographic materials, and explosives. However, lead can replace calcium in the skeletal system and accumulate. Exposure to lead (II) results in various neurodevelopmental effects, cardiovascular diseases, impaired renal function and fertility, hypertension, and adverse pregnancy outcomes [9]. The admissible limit for lead in drinking water is 0.01 mg/l [8].

Furthermore, Manganese (II) ion is the twelfth most abundant element and fifth most abundant metal on the earth. This metal has a silver-grey colour and is very easy to oxidise. Thus, Manganese (II) is not a free element; it usually exists as oxides, carbonates, and silicates. It is absorbed by ingestion, inhalation and dermal permeation and administered intravenously. It is rapidly absorbed in the gastrointestinal tract and lungs and then distributed into different tissues through blood circulation. The liver, pancreas, bone, kidney and brain are the organs containing the highest manganese levels in the human body [10]. The permissible limit for manganese (II) ions is 0.4 mg/l [8].

Adsorption using bentonite clay has been proven over the years to be a preferred method in water and wastewater treatment because of the simplicity of the process, coupled with the abundantly cheap supply of adsorbent, as well as the excellent properties which translate to outstanding and efficient removal of target pollutants [11]. Bentonites can adsorb a wide range of water pollutants due to their micron-size particles' large external and internal surface area [10]. The adsorption capacities of clay minerals have experienced significant improvement due to modification with quaternary ammonium compounds (QACs) [12]. Organoclays have progressively been used as adsorbents for heavy metal removal since they are cheaper than commercially available materials like zeolites and activated carbon [13]. The modification method involves altering the surface polarity of the clay minerals by intercalation with cationic surfactants [14, 15].

Bentonite clay offers an attractive and inexpensive option for removing inorganic and organic pollutants. The use of natural and modified bentonite for the adsorption of several heavy metals has drawn attention over the years [16]. The adsorption capacities of bentonite clay activated using different activation techniques are shown in Table 1.

Table 1 – Adsorption capacities of bentonite [16]

Modification / activation	BET, m^2/g	Pollutants/ Conc., mg/l	pH	Max. uptake, mg/g
Acid-thermal	109.85	Cr (III)/0.1	6	220
Natural	62.57	Pb (II)/200	7.4	51.9
Acid	-	Cr (VI)/20	3	4.22
Natural	-	Cu (II)/100 Cd (II)	-	7.94 7.64
Sulfate	73	Zn (II) Cu (II)/200 – 700	-	104.17 158.73
Phosphate	79	Zn (II) Cu (II)/200–700	-	111.11 166.67
Natural	23.5	Pb (II), Cd (II) and Mn (II)/10–50	6.6	9.32
Calcined	20.0	Pb (II), Cd (II) and Mn (II)/10–50	6.0	

Adsorption, like many other water and wastewater treatment methods, is a multi-factor dependent system whose efficiency can only be achieved when the independent variables such as pollutant load (usually in terms of initial concentration of the adsorbate (s)), adsorption time, temperature, dosage, and adsorbent particle size are chosen under favourable conditions. While many studies have been published on process optimisation using most of the listed criteria, the effect of particle size on the efficiency of surface processes has received less attention.

Response surface methodology is an optimisation tool that is very effective in determining the best conditions for a variety of processes, including adsorption [17, 18, 19, 20], chemical reaction integrated separation processes [21, 22, 23] and many others.

Therefore, this experiment was conducted not only to modify Dijah-Monkin bentonite clay with HDTMA-Br but also to determine the optimal particle size of the adsorbent, the initial concentration of each Pb, Cd, and Mn coexisting in the same solution, the adsorption time for maximum heavy metals removal efficiency, and the adsorption capacity of the synthesised adsorbent. The model solution for this study was synthesised using a known concentration of the considered metals.

METHODS

Preparation and Modification of Dijah-Monkin Bentonite Clay. This work used raw bentonite clay collected from the deposit site at Dijah-Monkin town in Zing LGA, Taraba State of Nigeria, subjected to preliminary treatment, beneficiated, modified with cationic surfactant HDTMA-Br, and characterised [24].

Adsorption Studies. All chemicals used are analytical-grade reagents. The multi-metal solution was prepared according to a procedure given by [16] to obtain 0.0048, 0.0089 and 0.0223 mole of lead (II), cadmium (II) and manganese (II) ion, respectively. The stock solutions were further diluted to desired concentrations of 10, 30 and 50 mg/l to mimic heavy metals concentrations in industrial effluents. The multi-metal solution (lead, cadmium and manganese) was obtained by mixing equal volumes of the known concentrations of the individual stock solutions where the particular concentration of the metals in the multi-metal solution retained their concentration as confirmed by atomic absorption spectrophotometer (Buck scientific model: VGB 210).

The sorption process involves mixing 50 mg of HDTMA-Br modified bentonite clay of selected particle size ranges in 50 ml of the multi-metal solution according to the design matrix. The supernatant was filtered using 110 mm diameter Whatman filter paper and analysed for metal ion residual concentration using the atomic absorption spectrometer (Buck Scientific model: VGB 210).

The adsorption capacity was calculated using the mass balance equation (Eq. (1)) [25].

$$q_e = \frac{(C_0 - C_e)V}{m} \quad (1)$$

where C_0(mg/l) and C_e(mg/l) are the initial and final (equilibrium) concentrations, respectively, V (l) is the volume of the solution treated, and m (g) is the mass of the adsorbent.

Furthermore, the percentage of heavy metal removal was obtained using Eq. (2) [25].

$$\%\ heavy\ metal\ removal = \left(\frac{C_0 - C_e}{C_0}\right) \times 100 \quad (2)$$

Design of Experiment with Response Surface Methodology (RSM). Design of experiment (DOE) is a well-accepted statistical technique that can design and optimise the experimental process. It involves choosing the optimal experimental design and estimating the effect of several variables independently and simultaneously interacting. Response surface methodology (RSM) is a statistical method used for experimental modelling and analysing the relationship between the input and response variables [26, 27, 28]. This study selected three process variables, particle size, initial metal ion concentration and contact time, to study the effect on adsorption capacity and percentage removal. Adsorption experiments were performed at selected level factors: particle size ranges of 50–150 μm, contact time of 30–180 minutes, and initial multi-metal concentration of 10–50 mg/l, as shown in Table 2.

Analysis of variance (ANOVA) was used to analyse regression coefficients, prediction equations, and case statistics. Diagnostics Plots and model graphs were obtained using Design Expert v.6.0.8 (Trial) to examine the effects of variables individually and their interactions to determine their

optimum level. The point prediction method was used to optimise the levels of each variable for maximum response.

Table 2 – Factors Level Selected for Adsorption Experiment

Factors	Code	Units	Level	
			Low	High
Particle Size	A	µm	50	150
Initial Concentration	B	mg/l	10	50
Contact Time	C	minutes	30	180

RESULTS AND DISCUSSION

Characterisation and Structural Formula of Modified Bentonite Clay. Oloyede et al. (2021) reported the XRD, FTIR, SEM, and XRF of the modified Dijah-Monkin bentonite clay. The XRF data were used to calculate the structural formula for the natural bentonite clay using the method presented by [24]. The calculation is presented in Table 3.

Table 3 – Calculation of Structural Formula for Modified Dijah-Monkin Bentonite Clay

Compound	Percent	Molecular weight	Cationic valency	Gram equivalent of cationic constituents	Cationic valence per unit cell	Cations per unit cell		Charge
SiO_2	63.44 ÷	60.04	× 4	= 4.227 ÷0.130	=32.48236 ÷4	8.1206 -0.1206 8.0000	tetrahedral group	- 0.1206
Al_2O_3	19.05 ÷	101.96	× 6	=1.121 ÷0.130	=8.6155 ÷3	(2.8718) 2.9924	octahedral group	-0.8756
TiO_2	0.71 ÷	79.9	× 4	=0.036 ÷0.130	=0.036 ÷4	0.0683		
Fe_2O_3	6.34 ÷	159.7	× 6	=0.238 ÷0.130	=1.831 ÷3	0.6102		
MnO	0.2 ÷	70.93	× 2	=0.0056 ÷0.130	=0.0433 ÷2	0.0217 3.6926		Composite layer charge -0.9961
				Sum(-Si and Al)	= 2.1471			
				Octahedral Al ×3	+8.9773 11.1244 -12.000 -0.8756	(Octahedral charge)		
CaO	1.04 ÷	56.08	× 2	=0.0371 ÷0.130	=0.2850 ÷2	0.1425	Interlayer cation charge	+0.6124
K_2O	2.88 ÷	94.20	× 2	=0.0611 ÷0.130 5.7252 5.7252÷44 = 0.130	=0.4699 ÷1	0.4699 0.6124		

Notes: Structural formula (half-cell)- $[(Al^{3+}_{1.49}\ Ti^{4+}_{0.03}\ Fe^{3+}_{0.31}\ Mn^{2+}_{0.01})^{-0.44}\ (Si^{4+}_{4.1}\ Al^{3+}_{0.06})^{-0.06}\ O_{10}(OH)_2]^{-0.50}(Ca^{2+}_{0.07}\ K^{+}_{0.24})^{+0.3}$

The structural formulas were in close agreement with the general molecular formula for the montmorillonite group, with silicon occupying all the tetrahedral sites. In contrast, aluminium occupied two-thirds of the octahedral sites. Potassium (K) and calcium (Ca) are exchangeable, and superscript "iv" is used to indicate tetrahedrally coordinated ions, while superscript "vi" is for octahedrally coordinated ions [12]. The general molecular formula of the montmorillonite group is $(Ca, Na, H)(Al, Mg, Fe, Zn)_2\ (Si, Al)_4O_{10}(OH)_{2-x}H_2O$.

The structural formula of the modified clay revealed the reduction of aluminium ions in the tetrahedral group. Furthermore, the exchangeable interlayer cations, such as calcium and potassium ions, also experienced a decrease, indicating more available sites for adsorption. The one-layer structural formula for modified clay in this study is $[(Al^{3+}_{2.99}\ Ti^{4+}_{0.07}\ Fe^{3+}_{0.61}\ Mn^{2+}_{0.02})^{-0.88}\ (Si^{4+}_{8.12}\ Al^{3+}_{0.12})^{-0.12}O_{20}(OH)_4]^{-1.00}(Ca^{2+}_{0.14}\ K^{+}_{0.47})^{+0.61}$

Box-Behnken Design (BBD). Table 4 presents the results of the responses (adsorption capacities and removal percentages) under different conditions (particle size, initial concentration, and contact time) from the design matrix using BBD.

The lead adsorption capacity (LAC) experimental result in Table 4 showed that the highest adsorption for lead removal was 49.98 mg/g at serial run 13. The lowest was 9.81 mg/g at serial run 10, while the lead percentage removal (LPR) was highest at 100% at serial run four and lowest at 98.07% at serial run 10.

The cadmium adsorption capacity (CAC) experimental result showed that the highest adsorption for cadmium removal was 49.41 mg/g at serial run 16, and the lowest was 9.77 mg/g at serial run 7.

Table 4 – Selected Factors and Responses for the Adsorption Experiment of Multi-Metal Solution

Run	Factors			Responses					
	Particle size, μm	Initial Concentration, mg/l	Time (minute)	Adsorption Capacity, mg/g			Percentage Removal, %		
	(A)	(B)	(C)	Pb	Cd	Mn	Pb	Cd	Mn
1	100.00	30.00	105.00	29.87	29.69	29.88	99.57	98.97	99.61
2	100.00	30.00	105.00	29.88	29.70	29.89	99.60	99.00	99.62
3	100.00	30.00	105.00	29.92	29.74	29.98	99.74	99.13	**99.93**
4	50.00	30.00	180.00	30.00	29.76	29.88	**100.00**	**99.20**	99.59
5	150.00	50.00	105.00	49.92	49.38	**49.96**	99.84	98.76	**99.93**
6	50.00	50.00	105.00	49.96	49.33	49.88	99.92	98.67	99.75
7	100.00	10.00	30.00	9.92	**9.77**	9.87	99.23	**97.70**	98.70
8	50.00	10.00	105.00	9.93	9.90	9.97	99.33	99.00	99.73
9	50.00	30.00	30.00	29.96	29.72	29.88	99.87	99.07	99.58
10	150.00	10.00	105.00	**9.81**	9.85	**9.86**	**98.07**	98.50	**98.60**
11	150.00	30.00	180.00	29.91	29.70	29.92	99.69	99.00	99.73
12	100.00	30.00	105.00	29.90	29.64	29.88	99.66	98.80	99.61
13	100.00	50.00	30.00	**49.98**	49.18	49.87	99.96	98.36	99.75
14	100.00	10.00	180.00	9.92	9.84	9.97	99.15	98.40	99.70
15	150.00	30.00	30.00	29.88	29.61	29.92	99.61	98.70	99.74
16	100.00	50.00	180.00	49.92	**49.41**	49.95	99.85	98.82	99.90
17	100.00	30.00	105.00	29.93	29.71	29.96	99.77	99.03	99.87

In contrast, the cadmium percentage removal (CPR) was highest 99.96% at serial run 13 and lowest 98.70% at serial run 10. The manganese adsorption capacity (MAC) experimental result showed that the highest adsorption for manganese removal was 49.96 mg/g at serial run 5. The lowest was 9.86 mg/g at serial run 10, while the manganese percentage removal (MPR) was highest 99.93% at serial runs 3 and 5; and lowest 98.60% at serial run 10. Many authors have also used CCD to analyse the adsorption data critically. Obtaining various values of responses at different levels of the factor combination in the design matrix indicated that the chosen 3-factor BBD adequately represented the adsorption system. In a recent investigation, CCD findings were obtained for pH, adsorbent dose, and initial concentration, with the maximum experimental removal of Cd^{2+} and Pb^{2+} being 98.90% and 99.99%, respectively [29].

Modelling and analysis of variance of adsorption capacity. To establish a mathematical relationship between each of the responses and the factors, the Fit Summary of the Design Expert 6.0.8 was used. The lead adsorption capacity ANOVA presented in Table 5 shows that the Model F–value is 1697439.16, which implies the statistical significance of the model with chances of error as low as 0.01%.

Also, based on a 95% confidence level, which gives an allowable error value to be equal to or less than 5%, the significant terms for the linear model developed are A and B. Values for the standard deviation (std.), mean, and correlation value (CV) were obtained to be 0.025, 29.92 and 0.084 respectively. Another coefficient of determination (R^2), adjusted R^2, predicted R^2 and adequate precision were also obtained to be 1.000, 1.000, 1.000 and 3293.114, respectively. The values of these parameters indicate the accuracy of the model.

Similarly, ANOVA results showed that the model developed for cadmium adsorption capacity was statistically significant with an F-value of 194975.95 and a p-value accounting for more than 99% confidence level. Moreover, these terms significantly affected the model because the p-values obtained for B, C, and B^2 were far less than the allowable probability of error (5%). Values for the std., mean, and CV were obtained to be 0.042, 29.64 and 0.14, respectively. In addition, the R^2, adjusted R^2, predicted R^2 and adequate precision were also obtained to be 1.000, 1.000, 1.000 and 1224.602, respectively.

Table 5 – Analysis of Variance for Adsorption Capacity

	Lead					Cadmium					Manganese				
Source	Sum of squares	Mean square	F value	Prob> F	Rmk	Sum of squares	Mean square	F value	Prob > F	Rmk	Sum of squares	Mean square	F-value	Prob > F	Rmk
Model	3204.47	1068.16	1.697 E6	< 0.0001	S	3208.23	1069.40	1.28 E6	< 0.0001	S	3199.50	1066.5	5.339 E5	< 0.0001	S
A	3.756E-3	3.75 E-3	5.97	0.0296	S	8.89 E-3	8.89E-3	10.63	0.0062	S	5.281 E-4	5.281 E-4	0.26	0.6158	
B	3204.47	3204.47	5.092 E6	< 0.0001	S	3208.21	3208.21	3.84 E6	< 0.0001	S	3199.5	3199.50	1.602 E6	< 0.0001	S
C	6.42 E-4	6.42 E-4	1.02	0.3309		0.023	0.023	13.01	0.0087	S	3.72 E-3	3.72 E-3	1.86	0.1955	
A^2						4.772 E-3	4.772 E-3	2.69	0.1453						
B^2						0.055	0.055	30.07	0.0009	S					
C^2						4.357 E-3	4.357 E-3	2.45	0.1614						
AB						2.336 E-3	2.336 E-3	1.13	0.2892						
AC						6.25 E-4	6.25 E-4	0.35	0.5718						
BC						6.400 E-3	6.400 E-3	3.60	0.0995						
Residual	8.18E-3	6.293 E-4				0.012	1.777 E-3				0.026	1. E-3			
Lack of Fit	5.486E-3	6.095E-4	0.90	0.5889	NS	7.119 E-3	2.373 E-3	1.78	0.2893	NS	0.017	1.886 E-3	0.84	0.3730	NS

Notes: *NS- Not Significant; *S- Significant; *Rmk – Remark.

The manganese adsorption capacity ANOVA shows a suggested Model F-value of 533895.56, which implies a significant model. In this case, B is the only considerable model term. Values for the std., mean, and CV were obtained to be 0.045, 29.91 and 0.15, respectively. Others were R^2, adjusted R^2, predicted R^2, and adequate precision, which were also obtained as 1.000, 1.000, 1.000, and 1846.868, respectively.

Table 6 summarises the model statistics of the adsorption capacity response with the suggested model.

Table 6 – Model Summary Statistics of Adsorption Capacity

Responses	Source	Standard deviation	R^2	Adjusted R^2	Predicted R^2	PRESS	Comments
Lead adsorption capacity	Linear	0.032	1.0000	1.0000	1.0000	0.023	Suggested
	2FI	0.032	1.0000	1.0000	1.0000	0.036	
	Quadratic	0.028	1.0000	1.0000	1.0000	0.048	
	Cubic	0.026	1.0000	1.0000		+	Aliased
Cadmium adsorption capacity	Linear	0.081	1.0000	1.0000	0.9999	0.16	
	2FI	0.087	1.0000	1.0000	0.9999	0.31	
	Quadratic	0.042	1.0000	1.0000	1.0000	0.12	Suggested
	Cubic	0.036	1.0000	1.0000		+	Aliased
Manganese adsorption capacity	Linear	0.045	1.0000	1.0000	1.0000	0.046	Suggested
	2FI	0.040	1.0000	1.0000	1.0000	0.044	
	Quadratic	0.046	1.0000	1.0000	1.0000	0.11	
	Cubic	0.047	1.0000	1.0000		+	Aliased

Accordingly, Pb, Cd, and Mn adsorption capacity data were respectively fitted to linear, quadratic, and linear models. After that, the obtained models were analysed for variance.

The final empirical model in terms of coded factors for LAC, CAC and MAC is given in Eqs. (3)–(5) respectively. A positive sign in front of the terms indicates a synergistic effect, whereas a negative sign indicates an antagonistic effect. The quality of the model developed was evaluated based on the correlation coefficient value. The R^2 value for these equations is 1.0000.

$$LAC = +29.91 - 0.033A + 20.03B - 0.008958C \quad (3)$$

$$(CAC)^2 = +29.70 - 0.022A + 19.74B + 0.054C + 0.0034A^2 - 0.11B^2 - 0.032C^2 + 0.024AB + 0.012AC + 0.040BC \quad (4)$$

$$MAC = +29.91 - 0.008125A + 20.00B + 0.022C \quad (5)$$

Figures 1, 2 and 3 represent the standard probability plot of the studentised form of residuals, which indicates whether the residuals follow a normal distribution, in which case the points will follow a straight line. In this study, the residues for LAC, CAC and MAC have a normal distribution

because the points follow the straight line with minimal variation from its direction. In this way, the proposed model's adequacy for observed data sets was confirmed.

The 3D view of the models was presented in Figures 4, 5, and 6 for LAC, CAC, and MAC, respectively, representing the linear interaction between the factors: initial concentration and particle size at a constant time of 105 minutes. The model graphs depict that the LAC, CAC and MAC increase in the initial concentration and larger particle size resulted in a higher adsorption capacity.

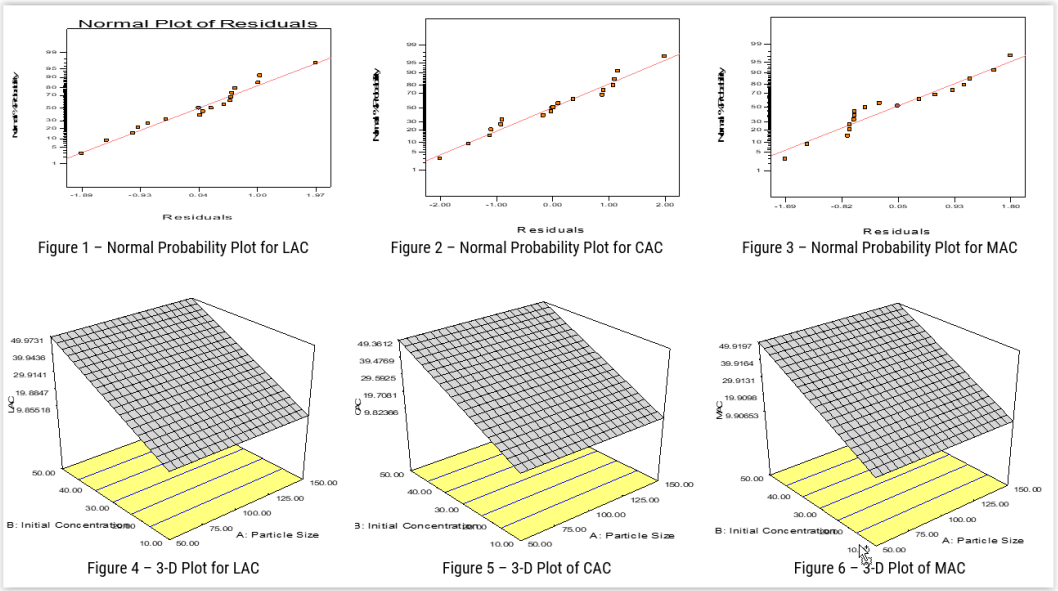

Figure 1 – Normal Probability Plot for LAC
Figure 2 – Normal Probability Plot for CAC
Figure 3 – Normal Probability Plot for MAC

Figure 4 – 3-D Plot for LAC
Figure 5 – 3-D Plot of CAC
Figure 6 – 3-D Plot of MAC

Notes: *LAC - Lead adsorption capacity, *CAC - Cadmium adsorption capacity, *MAC - Manganese adsorption capacity

Modelling and analysis of variance for percentage removal. The lead percentage removal ANOVA presented in Table 7 shows that the Model F-value was 27.18 for lead, which implied the model was significant with 0.01 % probability of error. A, B, B2, C2 and AB were the only considerable model terms in this model. Values for the std, mean, and CV were obtained as 0.081, 99.60 and 0.082, respectively. The R^2, adjusted R^2, predicted R^2 and adequate precision were obtained as 0.9722, 0.9364, 0.8145 and 19.324, respectively.

The cadmium percentage removal ANOVA suggested a Model F–value of 5.07, which implies a significant model. In this case, C and B^2 are the only considerable model terms. Values for the std., mean, and CV were obtained to be 0.21, 98.77 and 0.21, respectively. The R^2, adjusted R^2, predicted R^2 and adequate precision were obtained as 0.8669, 0.6958, 0.7438 and 1224.602, respectively.

Table 7 – Analysis of Variance for Percentage Removal

Source	Lead					Cadmium					Manganese				
	Sum of squares	Mean square	F value	Prob> F	Rmk	Sum of squares	Mean square	F value	Prob> F	Rmk	Sum of squares	Mean square	F value	Prob> F	Rmk
Model	1.62	1.62	27.18	<0.0001	S	1.92	0.21	5.07	0.0219	S	1.66	0.28	4.37	0.0201	S
A	0.11	0.11	16.34	0.0049	S	0.12	0.12	2.81	0.1373		0.054	0.054	0.84	0.3800	
B	1.15	1.15	173.4	< 0.0001	S	0.13	0.13	3.01	0.1263		0.84	0.84	13.19	0.0046	S
C	5.81E-3	5.808E-3	0.88	0.3801		0.32	0.32	7.54	0.0287	S	0.16	0.16	2.57	0.1399	
A2	3.89E-3	3.888E-3	0.59	0.4684		0.18	0.18	4.34	0.0757						
B2	0.20	0.20	29.97	0.0009	S	0.90	0.90	21.48	0.0024	S					
C2	0.041	0.041	6.21	0.0415	S	0.17	0.17	4.14	0.0814						

Source	Lead					Cadmium					Manganese				
	Sum of squares	Mean square	F value	Prob> F	Rmk	Sum of squares	Mean square	F value	Prob> F	Rmk	Sum of squares	Mean square	F value	Prob> F	Rmk
AB	0.11	0.11	17.13	0.0044	S	0.088	0.088	2.09	0.1914		0.43	0.43	6.72	0.0268	S
AC	7.61E-3	7.61E-3	1.15	0.3192		6.94E-3	6.94E-3	0.17	0.6967		6.94E-5	6.94E-5	1.1E-3	0.9743	
BC	2.25E-4	2.25E-4	0.034	0.8589		0.014	0.014	0.34	0.5769		0.18	0.18	2.86	0.1219	
Residual	0.046	6.62E-3				0.29	0.042				0.63	0.063			
Lack of Fit	0.016	5.46E-3	0.73	0.5857	NS	0.24	0.078	5.31	0.0702	NS	0.53	0.089	3.57	0.1193	NS

The manganese percentage removal ANOVA revealed a suggested Model F value of 4.37, which implies a significant model. In this case, B and AB are the only considerable model terms. The values for the std., mean, and CV were obtained to be 0.25, 99.61, and 0.25, respectively. The R^2, adjusted R^2, predicted R^2, and adequate precision were obtained as 0.7237, 0.5579, 0.1195, and 8.044, respectively.

Table 8 summarises the model statistics of responses with the suggested model. R^2 reflects the experiment's efficiency, while the adjusted and predicted R^2 are design expert software values.

Table 8 –Model Summary Statistics of Lead Percentage Removal

Responses	Source	Standard deviation	R^2	Adjusted R^2	Predicted R^2	PRESS	Comments
Lead percentage removal	Linear	0.18	0.7575	0.7015	0.5239	0.79	
	2FI	0.17	0.8303	0.7284	0.2588	1.23	
	Quadratic	0.081	0.9722	0.9364	0.8145	0.31	Suggested
	Cubic	0.087	0.9820	0.9281		+	Aliased
Cadmium percentage removal	Linear	0.36	0.2541	0.0820	-0.4343	3.17	
	2FI	0.39	0.3035	-0.1144	-2.0502	6.75	
	Quadratic	0.21	0.8669	0.6958	-0.7438	3.86	Suggested
	Cubic	0.12	0.9733	0.8932		+	Aliased
Manganese percentage removal	Linear	0.31	0.4589	0.3340	-0.0604	2.44	
	2FI	0.25	0.7237	0.5579	-0.1195	2.57	Suggested
	Quadratic	0.26	0.7963	0.5344	-1.6311	6.04	
	Cubic	0.16	0.9565	0.8260		+	Aliased

The standard deviation reflects the degree of deviation of the experimental from the actual value. The software suggested the quadratic model for LPR and CPR, while a two-factor interaction was suggested for MPR. The heavy metals percentage removal data were modelled based on the Fit Summary suggestions. Subsequently, analyses of variance for each of the models were carried out.

The final empirical model in terms of coded factors for LPR, CPR, and MPR is given in Eqs. (6)–(8), respectively.

$$(LPR)^{\square} = +99.67 - 0.12A + 0.38B - 0.027C - 0.030A^2 - 0.22B^2 + 0.099C^2 + 0.17AB + 0.044AC + 0.0075BC \quad (6)$$

$$(CPR)^{\square} = +98.99 - 0.12A + 0.13B + 0.20C + 0.21A^2 - 0.46B^2 - 0.20C^2 + 0.15AB + 0.042AC - 0.060BC \quad (7)$$

$$MPR = +99.61 - 0.082A + 0.32B + 0.14C + 0.33AB - 0.004167AC - 0.21BC \quad (8)$$

Figures 7, 8 and 9 represent the standard probability plot of the studentised form of residuals, which indicates whether the residuals follow a normal distribution, in which case the points will follow a straight line. In this study, the residues for LPR, CPR, and MPR have a normal distribution because the points follow a straight line with minimal variation in their direction. In this way, the proposed model's adequacy for observed data sets was confirmed.

Furthermore, the 3D view for the LPR depicts the relationship between initial concentration and particle size at a constant time of 105 minutes, shown in Figure 10. The model graph for the LPR shows that the increase in the initial concentration resulted in a higher percentage removal, while a higher particle size also increases the percentage removal. A slight increase in the per-

centage removal was observed, with the percentage removal approaching equilibrium as the concentration increased. In contrast, the increase in the particle size linearly enhanced the percentage removal.

The 3D view for the CPR, presented in Figure 11, shows that the percentage removal increased at lower concentrations and sharply declined as the concentration increased. Furthermore, the percentage removal reduced at shallow particle size and later increased as the particle size crossed 100 μm.

However, the 3D view of the model graph for the MPR, presented in Figure 12, shows that an increase in the initial concentration of manganese results in a higher percentage removal and increases steadily with an increase in the particle size.

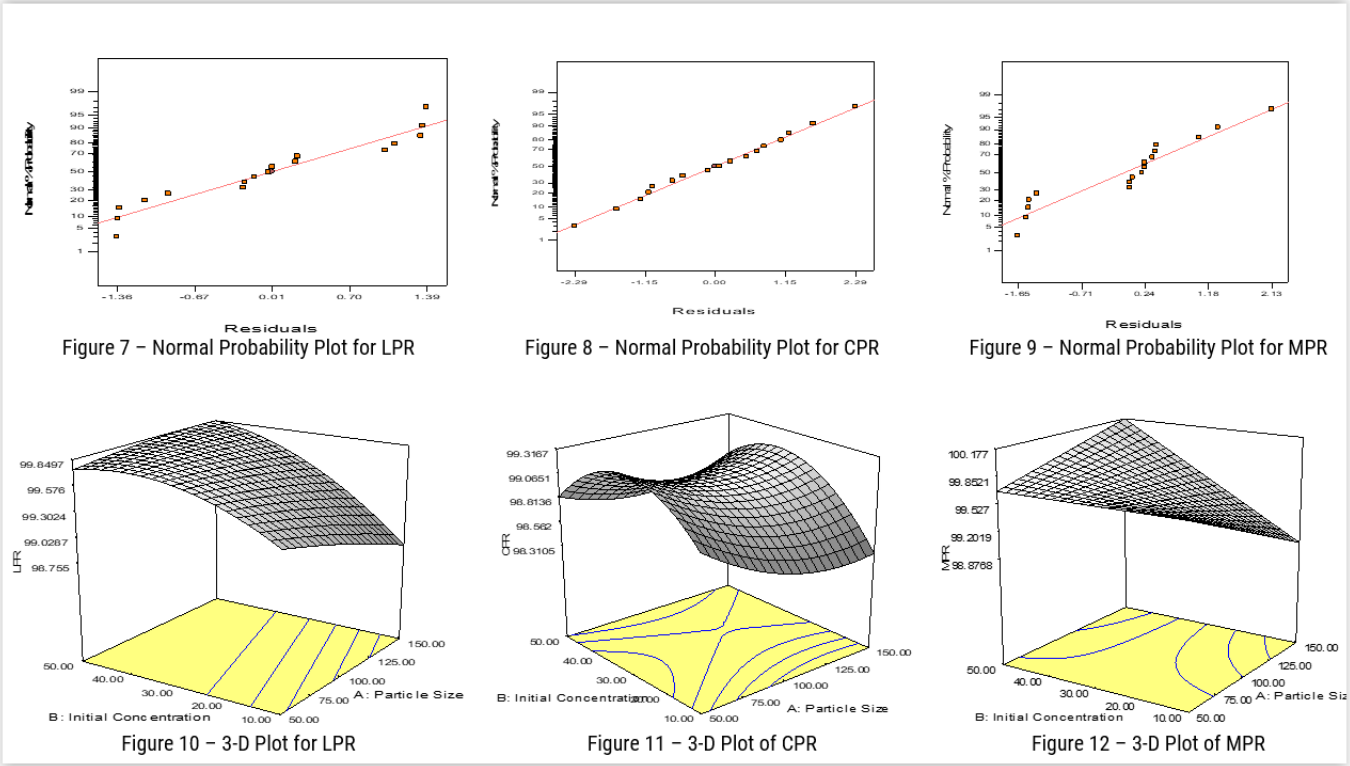

Figure 7 – Normal Probability Plot for LPR

Figure 8 – Normal Probability Plot for CPR

Figure 9 – Normal Probability Plot for MPR

Figure 10 – 3-D Plot for LPR

Figure 11 – 3-D Plot of CPR

Figure 12 – 3-D Plot of MPR

Notes: *LAC - Lead adsorption capacity, *CAC - Cadmium adsorption capacity, *MAC - Manganese adsorption capacity

Summary of Optimised Adsorption Capacity and Percentage Removal. The numerical optimisation method involved setting goals for each response to generate the optimal conditions. The optimisation goal was to maximise the adsorption capacities and percentage removal of the adsorbates, while the ranges of the factors were set as presented in Table 3. Table 9 shows the optimal adsorption limits for the adsorption capacity and percentage removal of the metals in the solution, while Table 10 shows the optimum condition suggested by the software.

Validation of the optimum condition. Adsorption experiments were carried out at the following optimum conditions (particle size 150 μm; initial concentration 50 mg/l and contact time 171 minutes) to validate the predicted optimisation results. The responses and their residuals are presented in Table 11.

Table 9 – Optimised RSM Values

No	Name	Goal	Lower limit	Upper limit
1	LAC	maximise	9.87	49.98
2	MAC	maximise	9.86	49.9633
3	CAC	maximise	9.77	49.41
4	LPR	maximise	98.7	99.96
5	MPR	maximise	98.6	99.9333
6	CPR	maximise	97.7	99.2

Table 10 – Optimal Point and Predictions

Particle Size (μm)	Initial Concentration (mg/l)	Time (min)	LAC (mg/l)	MAC (mg/l)	CAC (mg/l)	LPR (%)	MPR (%)	CPR (%)	Desirability
150.00	50.00	170.7	49.90	49.94	49.43	99.93	100	98.89	0.958
150.00	49.98	169.4	49.88	49.92	49.41	99.93	100	98.89	0.958
150.00	50.00	162.5	49.90	49.94	49.42	99.91	100	98.90	0.958
150.00	50.00	157.8	49.90	49.93	49.42	99.90	100	98.91	0.957

This result implies that the variation of the software-predicted values at the optimum point is minimal, which ascertains the accuracy of the results obtained from the optimisation.

Table 11 – Residuals of Validation of the Optimum Condition

№	Responses	Optimum value	Validation value	Residuals
1	LAC	49.90	49.832	0.0683
2	MAC	49.94	49.97	-0.0318
3	CAC	49.43	49.98	-0.5507
4	LPR	99.93	99.664	0.2689
5	MPR	100	99.94	0.0600
6	CPR	98.89	99.96	-1.0734

Comparison of optimal operating conditions. The suggested optimal values for lead, cadmium and manganese were almost similar to those proposed in other reported studies. Despite this, the values obtained differed, which shows that conditions were specific for each system according to the adsorbent characteristics, adsorbate type, and operating factors. A study conducted by [20] on the adsorption capacity of bentonite-kaolin-zeolite pellet in a multi-metal solution revealed 99.84% and 61.93% removal for lead and cadmium, respectively, which confirms the preferential removal of lead over cadmium. Another study on the adsorption capacity of zeolite by [30] revealed a 95.08% and 80.77% removal for lead and cadmium, respectively, while a study on the adsorption capacity of kaolin conducted by [31] for a multi-metal solution revealed a slightly different trend with 99.2% cadmium removal and 96.3% lead removal. The result of this study, however, agrees with the superior uptake of lead over cadmium in a multi-metal system. However, manganese experienced a higher uptake compared to both lead and cadmium, although the cation size indicated by the ionic radii increases from lead to manganese, i.e. 0.401, 0.426, 0.438 nm for Pb (II), Cd (II) and Mn (II) respectively [32] indicating that the smaller the cations, the faster their adsorption and the quantity adsorbed because they passed through the pores and channels within the bentonite structure with ease [33]. This deviation is probably due to the variation in operating factor time. Lead uptake is spontaneous and attains equilibrium early (about 30 mins). Still, though not sporadic, manganese uptake continues as the contact time increases, accounting for more uptake at 170 mins optimal time.

CONCLUSIONS

This research focuses on the optimisation of process parameters such as clay particle size (50–150 μm), metal ions initial concentration (10–50 mg/l) and contact time (30–180 minutes) for the maximum multi-metal adsorption capacity and percentage removal. The results of statistical analysis of the adsorption experiments carried out according to the Box-Behnken design showed that only the particle size and initial concentration had significant individual effects on the responses. However, the impact of contact time was substantial for cadmium removal, suggesting that the adsorption of cadmium ion on the adsorbent increases with increased contact time; this is due to high cadmium cation hydration energy of -1807 kJ/mol^{-1} compared to lead and manganese with -1481 $kJmol^{-1}$, -1760 $kJmol^{-1}$ respectively. Furthermore, the model equations for the responses were developed, and the optimum adsorption condition for the multi-metal adsorption that maximised the adsorption capacity and the percentage removal was obtained to be 150 μm particle size, 50 mg/l initial concentration over 171 minutes.

Acknowledgement

The authors would like to acknowledge financial support from Tertiary Education Trust Fund (TETFund) Institutional Based Research (IBR) (Ref. No: TETF/DR&CE/UNI/BAUCHI/IBR/2022/VOL.I).

REFERENCES

1. Kumar, D. (2015). *Preparation of Clay/Modified Clay Embedded Porous Hydrophobic Polymer for Removal of Pesticides and Heavy Metals from Water* (Master's thesis); Icar-Indian Agricultural Research Institute. Retrieved from https://krishikosh.egranth.ac.in/items/f5bd6c77-7547-452c-8955-3a1c96ad7b6e

2. Gautam, R. K., Sharma, S. K., Mahiya, S., & Chattopadhyaya, M. C. (2014). CHAPTER 1. Contamination of Heavy Metals in Aquatic Media: Transport, Toxicity and Technologies for Remediation. *Heavy Metals In Water*, 1–24. doi: 10.1039/9781782620174-00001

3. Duffus, J. H. (2002). Heavy metals-a meaningless term. *Pure and Applied Chemistry, 74*(5), 793– 807. doi: 10.1351/pac200375091357

4. Zhao, D., Jarinies, M., & Hasiao, B. S. (2010). Editorial for themed issue on "Advanced Materials in Water Treatments. *Journal of Materials Chemistry, 20*(22), 4476. doi: 10.1039/c005140n

5. Bhatnagar, A., Kumar, E., & Sillanpää, M. (2011). Fluoride removal from water by adsorption—A review. *Chemical Engineering Journal, 171*(3), 811–840. doi: 10.1016/j.cej.2011.05.028

6. Arora, R. (2019). Adsorption of Heavy Metals–A Review. *Materials Today: Proceedings, 18*, 4745–4750. doi: 10.1016/j.matpr.2019.07.462

7. Ahmad, K., Bhatti, A. I., Muneer, M., Iqbal, M. M., & Iqbal, Z. (2012). Removal of heavy metals (Zn, Cr, Pb, Cd, Cu and Fe) in aqueous media by calcium carbonate as an adsorbent. *International Journal of Chemical and Biochemical Sciences, 2*, 48–53.

8. Gebrekidan, M., & Samuel, Z. (2011). *Concentrations of heavy metals in drinking water from urban areas in Tigray region, Northern Ethiopia*. Retrieved from https://www.researchgate.net/publication/265809967_Concentration_of_Heavy_Metals_in_Drinking_Water_from_Urban_Areas_of_the_Tigray_Region_Northern_Ethiopia

9. Melichova, Z., Hromada, L. (2013). Adsorption of Pb2+ and Cu2+ ions from aqueous solutions on natural bentonite. *Polish Journal of Environmental Studies, 22*(2), 457–464.

10. Zhu, R., Chen, Q., Zhou, Q., Xi, Y., Zhu, J., & He, H. (2016). Adsorbents based on montmorillonite for contaminant removal from water: A review. *Applied Clay Science, 123*, 239–258. doi: 10.1016/j.clay.2015.12.024

11. Alexander, J. A., Ahmad Zaini, M. A., Surajudeen, A., Aliyu, E.-N. U., & Omeiza, A. U. (2017). Insight into kinetics and thermodynamics properties of multicomponent lead(II), cadmium(II) and manganese(II) adsorption onto Dijah-Monkin bentonite clay. *Particulate Science and Technology, 36*(5), 569–577. doi: 10.1080/02726351.2016.1276499

12. Aroke, U. O., Ibrahim, M., Osha, O. A., Yunus, M. H. (2015). Parametric studies of sulphate ion sorption at different pH on HDTMA-Br modified kaolinite clay. *International Journal of Emerging Trends in Engineering and Development, 3*(5), 250–260.

13. Abollino, O., Aceto, M., Malandrino, M., Sarzanini, C., & Mentasti, E. (2003). Adsorption of heavy metals on Na-montmorillonite. Effect of pH and organic substances. *Water Research, 37*(7), 1619–1627. doi: 10.1016/s0043-1354(02)00524-9

14. Jaynes, W. F., & Boyd, S. A. (1991). Clay Mineral Type and Organic Compound Sorption by Hexadecyltrimethlyammonium-Exchanged Clays. *Soil Science Society of America Journal, 55*(1), 43–48. doi: 10.2136/sssaj1991.03615995005500010007x

15. Wibulswas, R., White, D. A., & Rautiu, R. (1999). Adsorption of Phenolic Compounds from Water by Surfactant-Modified Pillared Clays. *Process Safety and Environmental Protection, 77*(2), 88–92. doi: 10.1205/095758299529857

16. Alexander, J. A., Ahmad Zaini, M. A., Surajudeen, A., Aliyu, E.-N. U., & Omeiza, A. U. (2018). Surface modification of low-cost bentonite adsorbents—A review. *Particulate Science and Technology, 37*(5), 538–549. 10.1080/02726351.2018.1438548

17. Rojas-Mayorga, C. K., Bonilla-Petriciolet, A., Aguayo-Villarreal, I. A., Hernández-Montoya, V., Moreno-Virgen, M. R., Tovar-Gómez, R., & Montes-Morán, M. A. (2013). Optimisation of pyrolysis conditions and adsorption properties of bone char for fluoride removal from water. *Journal of Analytical and Applied Pyrolysis, 104*, 10–18. doi: 10.1016/j.jaap.2013.09.018

18. Shittu, M. A., Aroke, U. O., Giwa, S. O. (2018). Response Surface Methodology for the Optimisation of Kerosene Desulphurization using Kaolinite Clay. *Nigerian Research Journal of Engineering and Environmental Sciences, 3*(2), 542–551.

19. Zbair, M., Anfar, Z., & Ahsaine, H. A. (2019). Reusable bentonite clay: modelling and optimisation of hazardous lead andp-nitrophenol adsorption using a response surface methodology approach. *RSC Advances, 9*(10), 5756–5769. doi: 10.1039/c9ra00079h

20. Carbonel-Ramos, D. E., Chirinos, H. D., Goméz-Marroquín, M. C., & Agarwal, M. (2021). Response Surface Methodology For Optimisation Of Heavy Metal Adsorption In A Multi-metal Solution By Bentonite-Kaolin-Zeolite Pellets. *Periódico Tchê Química, 18*(37), 57–75. doi: 10.52571/ptq-v18-n73-pgi.57-2021

21. Giwa, A., & Giwa S. O. (2012). Optimisation of transesterification reaction integrated distillation column using Design Expert and Excel Solver. *International Journal of Advanced Scientific and Technical Research, 2*(6), 423–435.

22. Giwa, A., & Giwa, S. O. (2013). Estimating the optimum operating parameters of olefin metathesis reactive distillation process. *ARPN Journal of Engineering and Applied Sciences, 8*(8), 614-624.

23. Mahmood, R. S., & Al-Musawi, N. O. A. (2020). Optimisation of Electrocoagulation Process for the TSS and Turbidity Removal in Al-Qadisiyah Water Treatment Plant in Baghdad City by Response Surface Methodology. *Key Engineering Materials, 870*, 97–105. doi: 10.4028/www.scientific.net/kem.870.97

24. Oloyede, O. G., Aroke, U. O., Giwa, S. O., & Jock, A. A. (2021). Characterisation of Natural and HDTMA-Br Modified Dijah-Monkin Bentonite Clay: FTIR, XRF, XRD and SEM. *Path of Science, 7*(5), 2010–2018. doi: 10.22178/pos.70-12

25. Hamadi, J. N., Mohammed, A. A., & Ali, A. H. (2014). Removal of Pb2+, Cu2+ and Cd2+ Metals from Simulated Wastewater in Single and Competitive System Using Locally Porcelanite. *International Journal of Engineering Sciences & Research Technology, 3*(7), 245–257.

26. Chong, M.-L., Abdul Rahman, N. A., Rahim, R. A., Aziz, S. A., Shirai, Y., & Hassan, M. A. (2009). Optimisation of biohydrogen production by Clostridium butyricum EB6 from palm oil mill effluent using response surface methodology. *International Journal of Hydrogen Energy, 34*(17), 7475–7482. doi: 10.1016/j.ijhydene.2009.05.088

27. Ferreira, S. L. C., Bruns, R. E., da Silva, E. G. P., dos Santos, W. N. L., Quintella, C. M., David, J. M., de Andrade, J. B., Breitkreitz, M. C., Jardim, I. C. S. F., & Neto, B. B. (2007). Statistical designs and response surface techniques for the optimisation of chromatographic systems. *Journal of Chromatography A, 1158*(1–2), 2–14. doi: 10.1016/j.chroma.2007.03.051

28. Bezerra, M. A., Santelli, R. E., Oliveira, E. P., Villar, L. S., & Escaleira, L. A. (2008). Response surface methodology (RSM) as a tool for optimisation in analytical chemistry. *Talanta, 76*(5), 965–977. doi: 10.1016/j.talanta.2008.05.019

29. Mohd Zahri, N. A., Md Jamil, S. N. A., Abdullah, L. C., Jia Huey, S., Nourouzi Mobarekeh, M., Mohd Rapeia, N. S., & Shean Yaw, T. C. (2020). Central composite design of heavy metal removal using polymer adsorbent. *Journal of Applied Water Engineering and Research, 9*(2), 133–146. doi: 10.1080/23249676.2020.1831978

30. Shaban, M., & Abukhadra, M. R. (2017). Geochemical evaluation and environmental application of Yemeni natural zeolite as sorbent for Cd2+ from solution: kinetic modeling, equilibrium studies, and statistical optimisation. *Environmental Earth Sciences, 76*(8). doi: 10.1007/s12665-017-6636-3

31. Malima, N., Lugwisha, E., and Mwakaboko, A. (2018). The efficacy of raw Malangali kaolin clay in the adsorptive removal of cadmium and cobalt ions from water. *Tanzania Journal of Science, 44*(2), 30–64.

32. Wang, X. S., Miao, H. H., He, W., & Shen, H. L. (2011). Competitive Adsorption of Pb(II), Cu(II), and Cd(II) Ions on Wheat-Residue Derived Black Carbon. *Journal of Chemical & Engineering Data, 56*(3), 444–449. doi: 10.1021/je101079w

33. Zendelska, A., & Golomeova, M. (2014). Effect of competing cations (Cu, Zn, Mn, Pb) adsorbed by natural zeolite. *International Journal of Science, Engineering and Technology., 2*(5), 483–492.